Global Change Biology (2002) **8,** 1253–1265

Effects of aggregated classifications of forest composition on estimates of evapotranspiration in a northern Wisconsin forest

D. S. MACKAY*†, D. E. AHL†, B. E. EWERS*, S. T. GOWER*, S. N. BURROWS*, S. SAMANTA* and K. J. DAVIS‡

**Department of Forest Ecology and Management, University of Wisconsin, 1630 Linden Dr., Madison, WI, 53706, USA, †Environmental Remote Sensing Center, Institute for Environmental Studies, University of Wisconsin, 1225 W. Dayton St., Madison, WI, 53715, USA, ‡Department of Meteorology, The Pennsylvania State University, 512 Walker Building, University Park, PA, 16802-5013, USA*

Abstract

Forest management presents challenges to accurate prediction of water and carbon exchange between the land surface and atmosphere, due to its alteration of forest structure and composition. We examined how forest species types in northern Wisconsin affect landscape scale water fluxes predicted from models driven by remotely sensed forest classification. A site-specific classification was developed for the study site. Using this information and a digital soils database produced for the site we identified four key forest stand types: red pine, northern hardwoods, aspen, and forested wetland. Within these stand types, 64 trees representing 7 species were continuously monitored with sap flux sensors. Scaled stand-level transpiration from sap flux was combined with a two-source soil evaporation model and then applied over a 2.5 km × 3.0 km area around the WLEF AmeriFlux tower (Park Falls, Wisconsin) to estimate evapotranspiration. Water flux data at the tower was used as a check against these estimates. Then, experiments were conducted to determine the effects of aggregating vegetation types to International Geosphere– Biosphere Program (IGBP) level on water flux predictions. Taxonomic aggregation resulting in loss of species level information significantly altered landscape water flux predictions. However, daily water fluxes were not significantly affected by spatial aggregation when forested wetland evaporation was included. The results demonstrate the importance of aspen, which has a higher transpiration rate per unit leaf area than other forest species. However, more significant uncertainty results from not including forested wetland with its high rates of evaporation during wet summers.

Keywords: eddy covariance, evapotranspiration, forested landscapes, hydrology, remote sensing, sap flux, spatial aggregation, vegetation classification

Received 15 February 2002; revised version received and accepted 14 June 2002

Introduction

Land surface process models are widely used to study water, carbon and energy at stand to regional scales, or as parameterization schemes in mesoscale and atmospheric global circulation models (GCM). Because species-level detail and finely resolved vegetation classification data are typically lacking, most prior studies aggregate in space and make simple assumptions about the similarity of species within a forest. With respect to modeling water and energy fluxes, the representation of vegetation has historically been either parameterized (e.g. Entekhabi & Eagleson, 1989; Wood *et al*., 1992), modeled in a rudimentary way (e.g. Deardorff, 1978; Pan & Mahrt, 1987), or mechanistically portrayed in terms of potential vegetation (e.g. Dickinson, 1984; Sellers *et al*., 1986, 1996; Pielke & Avissar, 1990; Avissar & Pielke, 1991; Foley *et al*., 1996, 2000; Xue *et al*., 1996). Improvements in vegetation modeling have in turn increased the demand

Correspondence: D. Scott Mackay, tel (608) 262-1669, fax (608) 262-9922, e-mail: dsmackay@facstaff.wisc.edu

for remote sensing based vegetation classification schemes. Some schemes, such as biosphere atmosphere transfer scheme (BATS) (Dickinson *et al*., 1998), SiB2 (Sellers *et al*., 1996), and International Geosphere–Biosphere Program (IGBP) (Loveland & Belward, 1997), emphasize vegetation structure; others are more functionally based (e.g. Running *et al*., 1995). To some extent all schemes recognize the need for functional grouping of vegetation. For example, different leaf longevity and surface resistance properties of conifer needle-leaf and deciduous broad-leaf species are routinely needed in land surface process models, and so these functional differences are incorporated into classification schemes (e.g. Running *et al*., 1995).

Since the vegetation classification schemes are model-driven they too focus on potential vegetation, which does not take into account earlier seral stages resulting from natural or human-based disturbance. When disturbance is considered it is because of a major shift in vegetation composition, such as conversion of forest to pasture or agricultural crops to urban (DeFries *et al*., 2000). These major changes are generally detectable from satellite imagery. Changes in forest composition can increase the spatial variability, especially of mixed stands, which can be beyond the ability of many satellite remote sensors to detect. Solutions to this problem have emphasized the mix of vegetated and non-vegetated areas (Moody, 1998) and differences in phenology among species (Wolter *et al*., 1995). The modeling community is using these advancements in remotely sensed classification procedures to improve estimates of leaf area index (LAI) and fraction of absorbed photosynthetically active radiation (e.g. DeFries *et al*., 2000; Pauwels & Wood, 2000; Zeng *et al*., 2000). Less attention is given to the problem of changes in vegetation type or LAI within a biome, which might arise as a result of forest management.

Forest management in northern Wisconsin and other regions of the world alters forest ecosystem structure and function. In northern Wisconsin, the forested vegetation composition is a reflection of the natural variability of drainage properties of different glacial landforms (Fassnacht & Gower, 1997, 1999) combined with the influences of over a century of forest clearing, succession and subsequent management. With respect to forest evapotranspiration, the assumption has been that natural and human-induced vegetation variability averages out at the landscape level. This allows for the aggregation of sub-grid spatial and taxonomic variability in vegetation parameterization. The purpose of this paper is to test this assumption in the context of predicting daily evapotranspiration from the forested landscape around the WLEF AmeriFlux tower in northern Wisconsin. With respect to natural variability we ask how much topographic variability, in particular the stratification of the landscape by upland and wetland, influences overall evapotranspiration. With respect to forest management we ask how much species level differences, in particular those relating to surface resistance, influence water fluxes.

We begin by producing a site-specific classification of forest composition, for use as a spatial framework for scaling stand-level flux measurements to the landscape, and as a taxonomic framework for aggregating from species-level to the IGBP vegetation classification (Loveland & Belward, 1997). Representative types of forest composition are then identified and detailed water flux measurements and modeling are made. Transpiration measurements at the stand level are combined with model estimates of upland soil and wetland soil evaporation, and aggregated to the landscape level. We then test for aggregation effects of including or excluding spatial variability in scaling up. Sensitivity tests are then conducted in which the taxonomic level of forest composition classification is varied to obtain alternate land surface parameterizations that reflect a loss of site-specific detail expected with global classification schemes.

Materials and methods

Site description

The study was conducted in northern Wisconsin, near Park Falls WI (45.945878 °N, 90.272304 °W). The study area was centred on a 447-meter tall communications tower instrumented to measure energy, water and carbon exchange between the forest landscape and the atmosphere (Bakwin *et al*., 1998; Berger *et al*., 2001). The tower and surrounding area is located in the Chequamegon-Nicolet National Forest. The area is situated in the Northern Highlands physiographic province, a southern extension of the Canadian Shield. The bedrock is comprised of Precambrian metamorphic and igneous rock, and overlain by 8–90 m of glacial and glaciofluvial material deposited approximately 10K to 12K years before present. Topography is slightly rolling with a range of 45 m within the defined study area. Outwash, pitted outwash, and moraines are the dominant geomorphic landforms. The growing season is short and the winters are long and cold. Mean annual July and January temperatures are 19 °C and −12 °C, respectively.

The forest vegetation reflects glacial topography (Fassnacht & Gower, 1997, 1999) and forest management activities, such as thinning, selective and clear-cut harvests. Red pine (*Pinus resinosa* Ait) and Jack pine (*Pinus banksiana* Lamb) dominate areas of excessively drained glacial outwash. Northern hardwood forests, comprised of sugar maple (*Acer saccharum* Marsh), red maple (*Acer rubrum* L.), green ash (*Fraxinus americana*), yellow birch

(*Betula alleghaniensis* Britton) and basswood (*Tilia americana* L.), occur in the finer textured moraines and drumlins. Intermediate sites support a wide variety of broadleaf deciduous tree species, such as paper birch (*Betula papyrifera* Marsh), quaking aspen (*Populus tremuloides* Michx), bigtooth aspen (*Populus grandidentata* Michx), red maple, and red and white pine (*Pinus strobus*). Poorly drained lowland sites are dominated by white cedar (*Thuja occidentalis* L.), balsam fir (*Abies balsamea* (L.) Mill), white spruce (*Picea glauca*), black spruce (*Picea mariana*), tamarack (*Larix laricina*), and speckled alder (*Alnus regosa*).

Site-specific classification

Land cover classes were derived using a site-specific classification scheme (Thomlinson *et al*., 1999), which allows for class aggregation up to the IGBP land cover classes. The site-specific classification has more detailed classes at the species level while the IGBP classification can be obtained by grouping these detailed classes. Ground-based measurements were initiated in 1998, in a 2.5 km × 3.0 km area surrounding the WLEF tower. A total of 312 permanent plots were established using a cyclic sampling scheme design based on the spatial variation of normalized difference vegetation indices derived from satellite remote sensing data (Burrows *et al*., 2002). A detailed description of the systematic design and inventory for each plot can be found in Campbell *et al*. (1999) and Burrows *et al*. (2002). All trees greater than 2.5 cm diameter at breast height (d.b.h) were identified using variable radius plots. Each plot was assigned to a site-specific class to enable aggregation up through the IGBP classification.

Airborne multispectral data was acquired with the NASA Airborne Terrestrial Applications Sensor (ATLAS) (Brannon *et al*., 1994) on September 8, 1998. ATLAS has 14 channels, of which six are similar in spectral bandwidth to Landsat Thematic Mapper (TM) and Enhanced Thematic Mapper (ETM+). Two flights at altitudes of about 1500 m and 7500 m, respectively, within a 2 h period near solar noon produced nominal ground resolutions of 3 m and 15 m. Prior to image acquisition, eight ground targets 6 m × 6 m in size were distributed throughout the study area to facilitate image geo-rectification. Coordinates for the targets were determined using differential Global Positioning System (GPS). Another 24 well-distributed points were collected after the flights at permanent plots near roads and other features recognizable on the imagery, such as road intersections. The relative accuracy of the GPS points was determined from a local survey benchmark to be within 0.5 m. Image coordinates were geo-referenced to the ground control points using a second order polynomial transformation. All images were resampled using a cubic convolution resulting in a root mean square (RMS) error of less than one pixel. It should be noted that this accuracy reflects RMS from the ground control points, which may not be representative of the registration accuracy for any given point in the image. Edges of flight lines can show more distortion because of the oblique angle of the scanner. We minimized this type of distortion by using the center 60% of the flight line. It is also true that along a lengthy flight line the platform geometry with respect to the ground surface can change. This can make it extremely difficult to construct a mathematical model to rectify a whole flight line. We minimized this problem by using only a 4 km long length of the flight line, which represents only a few seconds of flight time for the Learjet on which the ATLAS instrument is flown. These factors help to reduce the distortions caused by the side-scanning instrument and platform instability. We also qualitatively compared the rectified image to digital orthophotos, roads, and hydrography. Based on this assessment, well-distributed ground control points, and the fact that the terrain is relatively flat, the registration was considered adequate for landscape scale water flux estimates.

A hybrid classification approach was used to classify each 15 m pixel. A subset of the red, near infrared, mid-infrared bands, and a vegetation index was used in the analysis. First, wetlands were identified separately from uplands using the Wisconsin department of natural resources (DNR) wetland survey (WiDNR, 1998). To assist in refining the wetland/upland delineation further, digitized soils data were used to identify potential wetland; these sites were verified with repeated field visits to the permanent plots. All data sources were fused into the classification using heads up digitizing. Spectral training areas were selected from the imagery outside of the field plots and incorporated into unsupervised and supervised classification algorithms. We applied algorithms described by Lillesand & Keifer (2000), Stuckens *et al*. (2000), and Bauer *et al*. (1994) to identify spectrally unique signatures for each land cover class. Transformed divergence was used to evaluate the separability of classes and then input into a maximum likelihood classifier to assign each pixel in the image to a class. A post classification contextual analysis was applied to remove the 'salt and pepper' effect of independently classifying each pixel. Each pixel was assigned a majority land cover of the classes surrounding it (Stuckens *et al*., 2000) by resampling them to 5 m and then applying a 5 × 5 modal filter. The result was an assignment of majority land cover class per 25 m thus matching the nominal resolution of ETM+. As a test of the accuracy of the classification, the 312 permanent plots of Burrows *et al*. (2002) were used as an independent data set.

Water flux in forest stands

We measured sap flux in eight trees of each species in the following cover types: red pine, aspen/balsam fir, sugar maple/basswood, and forested wetlands consisting of speckled alder, white cedar and balsam fir. We identified stands with an average leaf area index (LAI) of 3.6 (with an actual range of 3.5–4.1 among the four stands). LAI was determined optically using a Li-Cor LAI-2000 Plant Canopy Analyzer (Li-Cor Inc., Lincoln, NE). In each forest type, 16 measurements were made in a 16 m radius of a canopy access tower at the center of each plot. The location of each measurement was recorded in order to analyze the means and standard errors spatially using the spatial statistics of Burrows *et al*. (2002). Standard field measurement methods were used to quantify L, including adjustments for clumping (Gower & Norman, 1991; Chen *et al*., 1997; Gower *et al*., 1999). Through soil texture analysis and soil maps we determined that our chosen stands were on the same soil types as the corresponding forest types within the site around the WLEF tower. Generally, upland conifer stands occur on loamy sands, deciduous stands occur on sandy loams, and forested wetlands occur with organic soils. Further details on site selection are given in Ewers *et al*. (2002).

We used Kucera-type sap flux sensors (Ewers & Oren, 2000) and Granier-type sap flux sensors (Granier, 1987) to obtain canopy transpiration. To avoid thermal gradients from direct radiation, all sensors were shielded with mylar. In each species of each stand, we scaled point measurements of sap flux to whole tree water flux per unit xylem area (J_S) using radial measurements through the conducting xylem and north and south circumferential measurements (Ewers *et al*., 1999, 2002; Ewers & Oren, 2000). In addition, we measured environmental conditions, including relative humidity and air temperature at 2/3 the average tree height, and photosynthetic photon density above the canopy. Transpiration was calculated by multiplying J_S by sapwood area per unit ground area (Oren *et al*., 1998; Ewers *et al*., 1999). For each stand, we calculated canopy transpiration, E_C, for each species and then summed up the transpiration for each day.

Water flux from the landscape

Three-axis sonic anemometers (Applied Technologies Inc., Boulder, Colorado, Model SAT-11/3K, or Campbell Scientific Inc., Logan, Utah, Model CSAT3, depending on date) are deployed at 30, 122, and 396 m above the ground to measure turbulent winds and virtual potential temperature. Air from each level is drawn down long tubes to the base of the tower where three infrared gas analyzers (IRGAs) (LiCor Inc., Lincoln, Nebraska, Model LI-6262) are used to determine CO_2 and water vapour mixing ratios at 5 Hz for E_C flux calculations. Berger *et al*. (2001) describe in detail how these flux data are obtained and processed. Observations of net radiation, photosynthetically active radiation, and rainfall provide supporting meteorological data. Profile observations were initiated in October of 1994, and flux observations began in May of 1995 (Davis *et al*., 2001). We used water flux data from the 122 m instrumentation. At this height, the average flux footprint lies within the region covered by our vegetation classification and field plots, assuming a ten-to-one ratio between instrument height and average fetch (Moncrieff *et al*., 1996).

For year 2000 data we selected a sub-sample of days corresponding to when our sap flux sensors were active (June 23–August 15). For years 1998 and 1999, days were selected from a period from May 20 through September 30. Our criteria for selecting days were as follows. First, observations were restricted to the leaf-on period in northern Wisconsin. Second, days that had a significant number of missing hourly flux values were not used. Here a significant number means more than one consecutive mid-day hourly flux measurement. However, more than one consecutive missing observation was accepted during low-light hours when latent heat fluxes were small and therefore not expected to contribute a large amount of error to the daily sum of evapotranspiration. Single missing observations during mid-day were corrected using accepted methods (Falge *et al*., 2001) when multiple days with similar light and vapour pressure deficit (VPD) conditions were available. When data from similar light and VPD conditions were not available to fill in gaps, we replaced the missing observation with the average of the fluxes from 1 h prior to and 1 h following the missing observation. This approach was used only when there were no large increases or decreases in light levels or VPD over the averaging time period. Hourly latent heat flux, LE [W m^{-2}] was converted to water depth equivalent flux-footprint evaporation for direct comparison to E_C. Hourly average LE was converted to an hourly water flux, E_h [mm h^{-1}] as follows:

$$E_h = \rho_w^{-1} \lambda_v^{-1} LE \quad (1)$$

where ρ_w is density of water and λ_v is the latent heat of vaporization, which was calculated as a function of air temperature measured at 122 m on the tower. Daily total tower water flux, E_{122}, was determined from E_h obtained over daylight hours as follows:

$$E_{122} = \sum_{i=\mathrm{bd}}^{\mathrm{ed}} E_h(i) \quad (2)$$

where bd and ed, respectively, refer to beginning of day and ending of day, which define daylight hours with an adjustment of timing such that the day begins when $E_h(i)$ changes from either a negative value or negligibly small positive value to positive and ends just prior to $E_h(i)$ turning negative or becoming negligibly small. Nighttime fluxes did not reliably go negative. However, diurnal periods with positive nighttime fluxes were usually eliminated because they corresponded to rainfall periods when the sap flux data were unreliable.

Vapor pressure deficit was determined using temperature and relative humidity in the Chequamegon red pine stand (Bruce Cook, *unpublished data*). This measurement was the most complete VPD record for the 1998 through 2000 period. To determine daily mean VPD, we retained only days when either the maximum recorded hour-averaged VPD exceeded 0.6 kPa, following a recommendation of Ewers & Oren (2000) or the daily average VPD was at least 0.2 kPa. Phillips & Oren (1998) suggest using 0.1 kPa as a minimum VPD for calculating daily canopy conductance; we selected 0.2 kPa to be conservative. Daily VPD was determined as an average of the hourly VPD values between a morning start time (bd) and an ending time (ed).

Soil evaporation

Given the amount of uncertainty involved in estimating soil evaporation over a large area, we chose to model it with a two-source soil resistance approach driven by available micrometeorological measurements. The first source was forest floor evaporation from the upland stands. The second source was forest wetland soil evaporation. We expect significantly greater evaporation from saturated forest soils, in wetlands or in uplands immediately after moderate to large rainfall events, and rapid decline in evaporation as the soil surface dries. A simple soil resistance scheme is sufficient to capture the wetting and drying dynamic in the upland forests with relatively small error for estimating evaporation in our case, as wetlands represent about 40% of the area and there were relatively few days of rain of sufficient quantity to wet the forest floor. The soil surface evaporation fluxes were determined using a soil resistance formulation (Mahfouf & Noilhan, 1991):

$$E_S = \frac{\rho_a c_p [e_{sat}(T_s) - e_a]}{\rho_w \lambda_v \gamma (R_{soil} + R_a)} \ (\mathrm{m}) \qquad (3)$$

where ρ_a and ρ_w are, respectively, air and water density, c_p is specific heat of air, γ is the psychrometric constant, R_{soil} and R_a are, respectively, soil and aerodynamic resistance, and $e_{sat}(T_s) - e_a$ represents the vapour pressure difference between the soil surface and the air. Data from a mixed stand (Bruce Cook, unpublished data) was used for upland meteorological conditions; a combination of data from two wetland stands (Bruce Cook, unpublished data; Ewers *et al*., 2002) was used for wetland soil evaporation. We chose the mixed stand to represent upland soil evaporation because of its moderately higher soil water content than the pine stand, which occurs on well-drained soils. The mixed stand was believed to be more conservative for estimating order-of-magnitude upland soil evaporation rates, and it is the most common upland forest type in the study area. R_{soil} was calculated according to Camillo & Gurney (1986) as

$$R_{soil} = 4104(\phi - \theta) - 805 \qquad (\mathrm{s\ m^{-1}}) \qquad (4)$$

where ϕ is soil porosity obtained by using the soils map and standard lookup tables (Clapp & Hornberger, 1978), and θ is near surface (top 5 cm) volumetric soil moisture content. Temperature and humidity were measured at 2.6 m above the soil surface (and below forest canopy). For the wetland soils it was assumed that $\theta = \phi$. For both below forest conditions, R_a, was calculated using the correction for air stability due to temperature stratification (Daamen & Simmonds, 1996; Baldocchi *et al*., 2000)

$$R_a = \frac{[\ln(z/z_0)]^2}{k^2 u}(1+\delta)^{\varepsilon} \qquad (\mathrm{s\ m^{-1}}) \qquad (5)$$

where z and z_0 describe the height of the near surface layer and roughness length of the soil, respectively, k is von Karman's constant (0.40), u is wind speed, and ε is a coefficient, which was set to -0.75 when δ was positive and -2 when δ was negative (Baldocchi *et al*., 2000). Wind speed was taken from a mixed forest stand for both upland and wetland calculations, as the instrumentation in the wetland was not functioning properly for most of the period of this study. The dimensionless term, δ, is calculated as

$$\delta = \frac{5gz(T_s - T_a)}{T_a u^2} \qquad (6)$$

where T_s and T_a are soil surface and air temperatures, and g is the acceleration due to gravity.

Aggregating from stand to the landscape

Using data from the WLEF tower we calculated a daily mean wind direction. The area around the tower was divided into quadrants each approximately 1.5 by 2.0 km in size, or the equivalent of three cells of 1 km^2 resolution remote sensing sensors. One or two upwind quadrants were determined for each day based on the wind direction. The full area of each quadrant was used

in calculating a weighted sum of evapotranspiration based on our sap flux measurements and soil evaporation estimates. Weights were obtained from the site-specific vegetation classification map. In calculating the weighted average fluxes open wetlands were grouped with forested wetland, the mixed category was divided equally among the four major forest types, and grass/disturbed and road were ignored. Note that the upland grass area around the tower is too small to contribute substantially to the scalar source area for flux measurements made at 122 m.

Results and discussion

Figure 1 shows the site-specific classification map. Overall accuracy is 84% when compared with the independent 312 ground truth plots. The percentage of ground truth plots correctly classified were 79 in aspen, 93 in forested wetlands, 55 in red pine and upland conifer, and 93 in northern hardwoods. Two key properties of our site-specific classification are that (1) site-specific classes can be aggregated to form IGBP vegetation classes and (2) site-specific classes can be disaggregated to identify representative species for ground-level flux measurements. We identified four dominant forest composition types (forested wetland, hardwoods, pine and other conifers, aspen) representing 86% of the area covered by our site-specific classification. Within each forest type, the most representative species (Fig. 2) were identified based on their relative basal area (Burrows *et al.*, 2002). Figure 2 shows the hierarchical framework used to extrapolate ground-based measurements to the landscape around the tower using either the site-specific or IGBP classes. This framework allows for a more detailed level to nest both spatially and taxonomically into the next most aggregated level. This is consistent with any consideration of ecosystem functioning (Franklin & Woodcock, 1997; Thomlinson *et al.*, 1999).

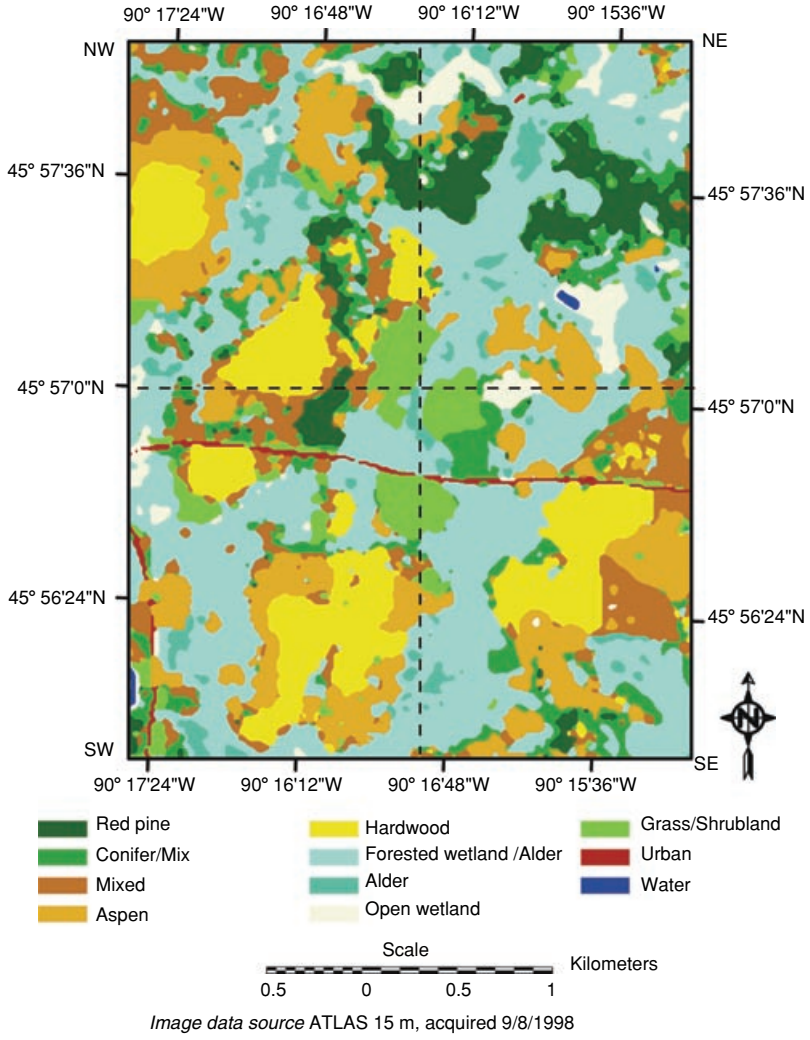

Fig. 1 Site-specific land-cover classification for area around the WLEF tower. The four quadrants (NW, NE, SE, SW) each cover an area of 3.6 km^2.

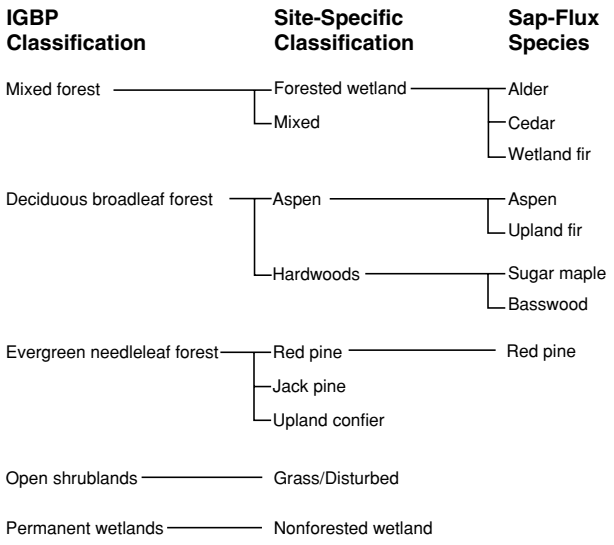

Fig. 2 A three-level classification system for the landscape around the WLEF tower. Species are aggregated to form site-specific cover types, which are in turn aggregated to obtain International Geosphere–Biosphere Program (IGBP) classes.

In forest stands selected to be representative of our site-specific classification, Ewers *et al*. (2002) found the following: (1) Variation in daily E_C was best explained by exponential saturation curves in response to daily average VPD; (2) the highest E_C was found in aspen/fir averaging 2.0 mm day^{-1}; and (3) the lowest E_C occurred in northern hardwoods averaging 0.9 mm day^{-1}. LAI ranged from 3.5 m^2 m^{-2} in the aspen stand to 4.1 m^2 m^{-2} in the forested wetland stand. Such variation is too small to explain the differences in E_C rates among stands. The low rates in northern hardwoods could be explained by a low canopy average stomatal conductance in sugar maple and basswood. Another possibility is that the thinning that occurred in northern hardwoods stands around year 1990 has reduced the LAI lower than is typical for mature forest of this type. High E_C in aspen is expected given its high growth rate and commensurate high demand for water. Oren *et al*. (1999) showed that large differences in sap flux are supported across a wide range of species that regulate their water potential to prevent runaway cavitation, and Ewers *et al*. (2000) explained this stomatal behavior in terms of vulnerability to cavitation.

Table 1 summarizes all transpiration fluxes by stand and evaporation fluxes by topographic position. Evaporation from wetland soils is generally higher than any of the transpiration rates and is typically an order of magnitude greater than the upland soil evaporation. There is also a large variation among days for both soil evaporation fluxes, as would be expected given their proportionality to VPD (Eq. 3), which had daily mean values in the range of 0.3–1.6 kPa. In general, radiation levels are too low below forest copies with LAI between 3 and 4, and as such contribute little to evaporation. The dependence of the soil evaporation fluxes on R_{soil} and R_a disserve some discussion. First, R_{soil} tends to be either negligibly small in the saturated soils of the wetlands or large in the drier upland soils. Summer precipitation is typically small enough that most of the water is intercepted on the forest canopy and little of it recharges the soils. This is born out in the 5 cm soil moisture data during summer 2000. In general, the upland soil evaporation fluxes are small enough that this uncertainty contributes negligibly to overall fluxes from the landscape. Second, R_a is a difficult term to quantify and there is little data under vegetation that does so (see Baldocchi *et al*., 2000 for a review). Baldocchi *et al*. (2000) showed that the stability correction for temperature stratification (Eq. 5) was important for sensible heat flux, but less important for latent heat flux under forest canopies. The remaining unknown in Eq. 5 is the roughness length (z_0), but this has been shown to be only weakly dependent on wind speed (Sauer *et al*., 1996; Campbell & Norman, 1998). Further measurements and sensitivity analyses are needed to increase our confidence in soil flux measurements at any given location, but this level of detail would become increasingly difficult to defend as we scale from the stand to the landscape.

Figure 3 shows E_{122} for days obtained from 1998, 1999, and 2000 eddy covariance data. Also shown is a weighted average of sap flux calculated by taking the sum of stand-level E_C multiplied by proportion of the study site covered by the respective stand types. Exponential saturation curves are used to fit all data shown, although the 1999 and 2000 E_{122} could arguably be plotted as linear functions of VPD. E_{122} for 1998 shows a response more like that of the sap flux data. The saturating curve for transpiration follows from the well-known stomatal closure response to high VPD (Jarvis, 1976; McNaughton & Jarvis, 1991; Monteith, 1995), which in fact is a surrogate for the regulation of water potential through the conducting pathways of the plants (Sperry *et al*., 1998; Oren *et al*., 1999; Meinzer *et al*., 2001). Ewers *et al*. (2002) report that transpiration from all four sap flux stands was explained primarily by VPD, while soil water, measured in each stand, had no influence on transpiration at any time during the year 2000 measurement period. The near-linear E_{122} to VPD responses can either be attributed to a large evaporation component flux from a wet canopy or evaporation from saturated soils. These fluxes are limited primarily by the aerodynamic properties of the surface. In our study, sap flux measurements are reported for days with minimal rainfall. Thus, if upland soil evaporation is sufficiently small, then a remaining working hypothesis is that E_{122} is dominated at high VPD by evaporation from wetland soils below

Table 1 Year 2000 water flux numbers (mm day^{-1}) per unit ground area, organized by stand transpiration or soil evaporation. Transpiration numbers are derived from sap flux measurements scaled by sapwood area and divided by stand ground area for each respective stand. Soil evaporation fluxes are derived using Eqs (3–6) with inputs of temperature, humidity, and wind speed from the mixed (upland) and forested wetland (lowland) micrometeorological stations near the WLEF tower. The numbers shown in bold were filled using regression against other species transpiration data, as follows. Upland fir was regressed with aspen, wetland fir with cedar, maple and basswood with aspen, and alder with maple. To obtain a landscape level total evapotranspiration: (1) sum up flux values for species within each stand, (2) multiply each stand level flux with the proportion of its respective cover type (i.e. row totals in Table 2), (3) multiply upland and wetland soil fluxes by the proportion of upland and wetland area, respectively, and (4) sum the weighted flux numbers

	Conifer		Aspen/Fir		Forested wetland		Northern hardwoods		Soil evaporation	
Day	Red Pine	Aspen	Fir	Cedar	Fir	Alder	Maple	Basswood	Upland	Wetland
173	0.39	1.17	0.03	0.18	0.02	**0.68**	0.46	0.14	0.00	0.00
174	0.31	0.67	0.03	0.11	0.01	**0.42**	0.28	0.04	0.00	0.00
175	0.89	1.82	0.08	0.41	0.03	**0.92**	0.62	0.15	0.10	1.23
176	1.11	2.36	0.10	0.47	0.03	**0.96**	0.65	0.25	0.32	6.24
178	1.42	3.29	0.18	0.73	0.04	**1.15**	0.78	0.27	0.23	2.70
179	0.95	1.93	0.10	0.52	0.03	**0.93**	**0.63**	**0.24**	0.03	0.55
180	1.29	3.00	0.17	0.72	0.05	**1.14**	**0.77**	**0.37**	0.17	4.33
192	1.81	3.06	0.12	0.74	0.04	**1.15**	0.77	0.29	0.86	5.95
194	0.49	0.80	0.04	0.18	0.01	**0.42**	0.28	0.06	0.03	0.55
195	1.77	2.95	0.11	0.66	0.04	**1.11**	0.75	0.29	0.28	6.72
196	1.90	3.12	0.11	0.70	0.04	**1.11**	0.75	0.28	0.18	5.42
197	1.80	3.18	0.11	0.70	0.04	**1.11**	0.75	0.27	0.15	5.50
198	1.94	3.00	0.10	0.69	0.04	**1.20**	0.81	0.30	0.14	6.01
199	1.72	2.73	0.10	0.68	0.04	**0.97**	0.65	0.27	0.08	3.45
200	1.15	1.67	0.06	0.43	0.02	**0.77**	0.52	0.11	0.00	0.01
202	1.11	1.80	0.08	0.43	0.03	1.06	0.55	0.19	0.03	1.58
203	1.07	1.33	0.07	0.37	0.02	0.65	0.52	0.14	0.00	0.00
204	1.42	2.00	0.09	0.47	0.03	1.15	0.68	0.22	0.03	2.07
205	1.84	2.47	0.09	0.48	0.03	1.26	0.86	0.28	0.09	5.93
209	0.87	0.87	0.03	0.21	0.01	0.49	0.28	0.14	0.01	0.00
210	0.90	1.01	0.06	0.21	0.02	0.43	0.36	0.13	0.09	0.27
211	1.94	2.41	**0.10**	0.53	**0.03**	1.21	0.81	0.35	0.32	4.63
213	2.49	2.35	0.11	0.52	0.03	1.22	0.81	0.37	0.16	5.57
215	1.44	2.09	0.10	0.50	0.03	1.21	**0.66**	0.25	0.03	0.55
216	1.71	2.01	0.08	0.50	0.02	1.06	0.75	0.27	0.09	2.64
218	1.18	1.17	0.09	0.33	0.03	0.43	0.47	0.17	0.00	0.17
219	1.20	1.10	0.09	0.29	0.03	0.66	0.44	0.17	0.03	1.26
220	2.15	2.11	0.07	0.52	0.02	1.18	0.80	0.34	0.24	2.03
222	1.47	1.48	0.11	0.41	0.04	**0.78**	**0.52**	0.24	0.08	0.89
223	2.11	2.24	0.05	0.49	0.02	**1.32**	0.89	0.33	0.27	5.73
226	1.77	1.80	0.10	0.47	0.05	**1.09**	0.74	0.27	0.13	3.97

forest canopy. As one would expect the importance of the forested wetlands increases under high VPD conditions.

The fluxes in Table 1 should be thought of as sources that are mixed by atmospheric turbulence and observed in aggregate via the 122 m eddy-covariance system. Sources of fluxes, aggregated according to wind direction at the WLEF tower, are given in Table 2. With the exception of the NW quadrant, all major forest types are reasonably well represented in all areas. Figure 4 shows a comparison of the weighted total flux estimates and the water flux observed at the tower. With the exception of a slight positive bias, the combination of transpiration and soil evaporation components explains most of the linear E_{122} response to VPD. Alternatively, using weighted total fluxes based on the whole region around the tower produced a similar intercept, and based on an analysis of variance the difference between the regression slopes is not significant ($\alpha = 0.05$). This indicates that the forest types are spatially well mixed in the region around the WLEF tower. We attribute this result in part to the

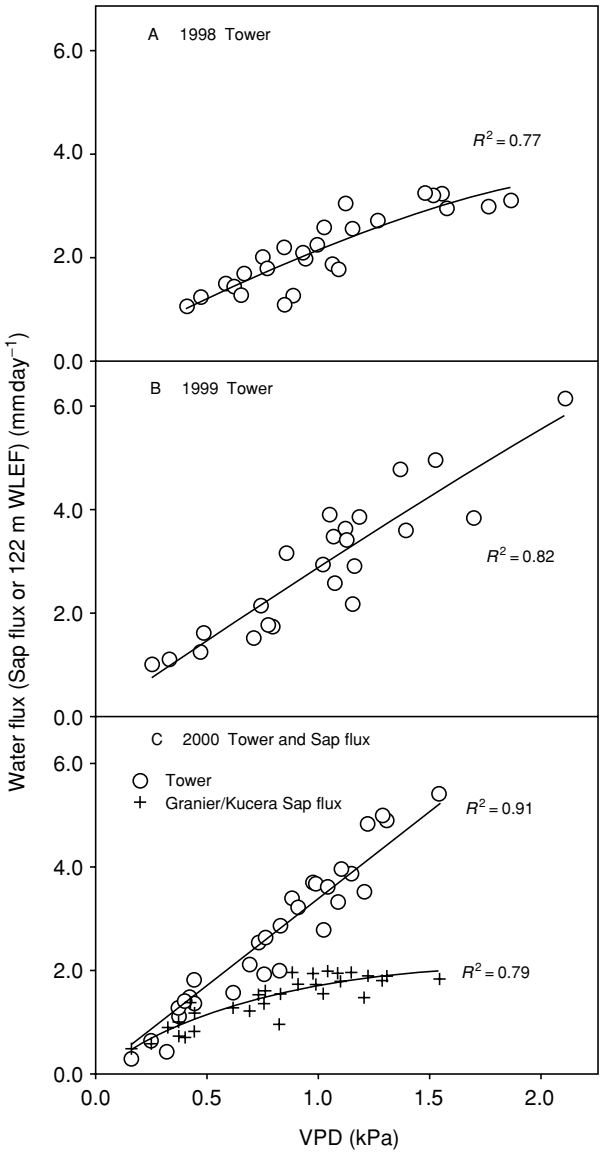

Fig. 3 Water flux measurements acquired at the WLEF tower (122 m) and from a weighted average from sap flux based on percent coverage for whole study area.

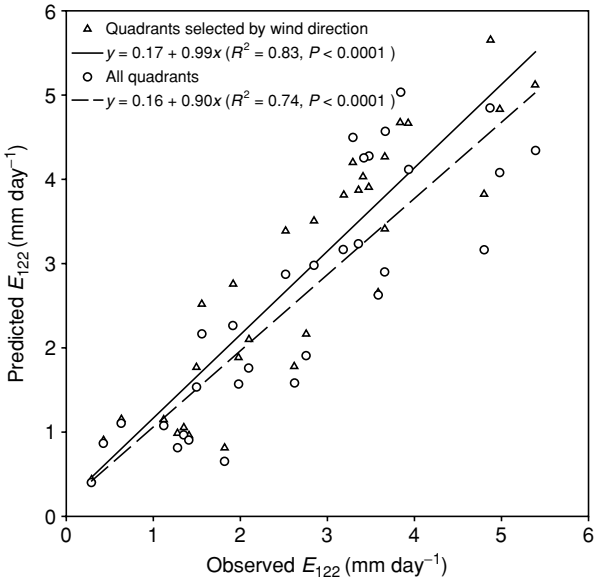

Fig. 4 This graph shows a comparison between predicted and observed evapotranspiration at the WLEF tower 122 m level eddy covariance using wind direction to select quadrants (△) and using all quadrants (○). Based on ANOVA, the two regression slopes are not significantly different from each other.

Table 2 Cover types by percentage of each quadrant of the region shown in Fig. 1

	Percent coverage by quadrant			
Cover type	NE	NW	SW	SE
Maple-basswood	0.89	13.41	14.36	15.40
Aspen	12.49	18.27	11.36	18.76
Red pine/Conifer	23.59	11.91	3.64	2.11
Forested wetland	41.33	26.15	41.96	37.54
Open wetland	7.01	3.31	5.50	1.30
Grass/Disturbed	9.51	9.61	11.75	3.70
Mixed	5.13	17.00	9.70	20.08
Road	0.05	0.34	1.72	1.10

glaciated landscape of northern Wisconsin, with its repetitive patterns of low-lying outwash plains and uplands of ice-contact materials. The natural setting gives rise to variable drainage conditions that support different forest types. However, superimposed on the natural setting is forest management, which plays a major role in shaping the distribution of forest composition. We must be cautious in generalizing about these results for other parts of northern Wisconsin and other regions, where land use and land cover patterns are different. It is also important to keep in mind that our study area is 40% forested wetland, and during year 2000, the summer months were much wetter than normal. A linear E_{122} response to VPD would not necessarily be expected if there was significantly less saturated soil surface area, as might occur in other areas in northern Wisconsin and elsewhere, or even at the WLEF site in a dry year (e.g. 1998 as shown in Fig. 3a). If drier conditions result in a very different spatial distribution of saturated soils associated with lower regional groundwater table heights, then the difference between directional and total landscape estimates of E_{122} would have to be reconsidered.

When forest transpiration is a dominant part of the surface to atmosphere flux then an exponential saturation

curve with VPD is expected. Alternatively, free evaporation from open water, saturated soils and wet canopies should occur at a linear or greater rate with VPD. A saturating response could result from soil resistance during a dry period when upland soil surface moisture content is low and VPD levels are high. However, evaporation from soils under these conditions would contribute a negligible flux. Based on this argument we suggest that the 1998 summer tower fluxes are dominated by forest transpiration (Fig. 3a). The June and July period during 1998 was much drier than normal. During our first field campaign to establish permanent field plots we observed that the wetlands were relatively dry with overall less saturated soil surface area. Since wetland conditions are strongly controlled by topography and seasonal water table levels dictate CH_4 vs. CO_2 fluxes across a topographic gradient (Waddington & Roulet, 2000), we hypothesize that it may be possible to corroborate water flux estimates at WLEF by looking at CH_4:CO2 ratios. For example, at WLEF, the late summer 1998 drought appears to have significantly reduced methane fluxes during the spring of 1999 (C. Werner, unpublished data). A combined analysis of the interactions between water table, ET, CO_2 fluxes and CH_4 fluxes is clearly a topic for future research.

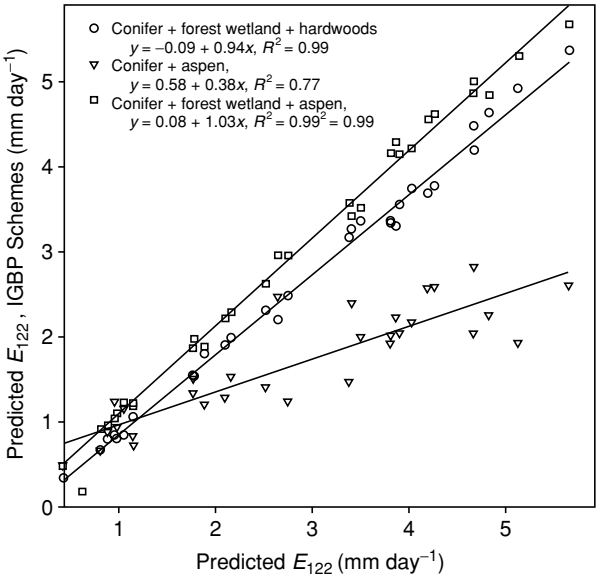

Fig. 5 Comparison of predicted 122 m tower footprint evapotranspiration results using (□) aspen to represent deciduous broadleaf in a site-specific classification, (▽) using hardwood stand to represent deciduous broadleaf, and (○) using conifer and aspen to represent biome-specific parameterization. The conifer and aspen combination is an approximation of IGBP mixed forest category with no knowledge of permanent wetlands.

By including or excluding different species level flux numbers and wetland evaporation different taxonomic levels of aggregation can be simulated. Figure 5 shows predicted water flux from three such aggregation schemes in comparison to the prediction using quadrant selection and complete site-specific flux numbers. In two of the cases, an IGBP mixed forest class was approximated, but augmented with knowledge of permanent wetland under the forest canopy. It was assumed that the forest composition consisted of 50% conifer, with water flux represented by red pine transpiration, and 50% deciduous broadleaf. In one case, the deciduous water flux was represented by northern hardwood transpiration, and in a second case, it was represented by aspen transpiration. In northern Wisconsin, hardwoods and aspen represent the low and high end of transpiration flux, respectively (Ewers *et al*., 2002). For the third test, we assumed an IGBP mixed forest category with no knowledge of wetland and an even mix of red pine and aspen (Fig. 6). While a number of different combinations were possible, we felt these three effectively illustrated the range of variability associated with retaining or losing topographic control (uplands or wetlands) and uncertainty associated with selecting a representative deciduous species type. Biome-based classifications, such as Running *et al*. (1995), have deciduous and conifer classes, but do not include a forested wetland class. Furthermore, a sensitivity analysis by Ahl (2002) on model input parameters for RHESSys (Mackay & Band, 1997; Mackay,

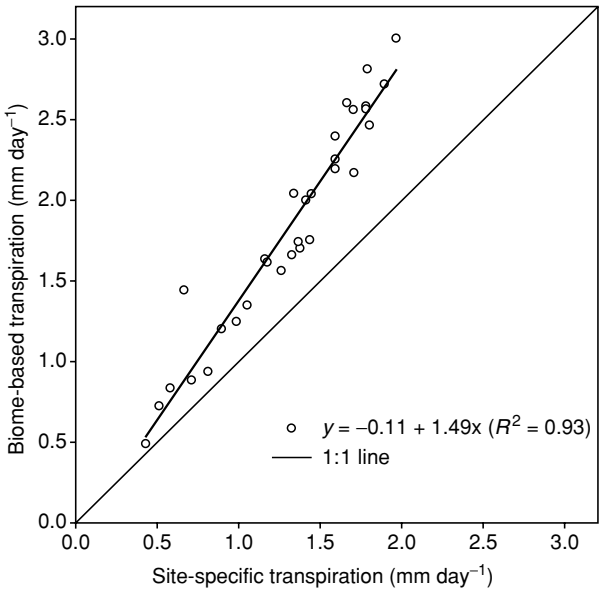

Fig. 6 Comparison of the site-specific (species level) transpiration estimated to contribute to the 122 m tower footprint water flux to transpiration based on biome-specific parameters (conifer and deciduous level).

2001), showed that red pine and aspen corresponded closely in terms of parameters with typical conifer and deciduous BIOME-BGC (Running & Hunt, 1993) parameters, respectively. The result clearly shows that water flux from the forested wetland is key to predicting overall water flux for the relatively wet conditions of our study period. Even including the high transpiration rate of aspen is small in comparison to flux underestimation that results from ignoring the forested wetlands. An IGBP classification that retains a forested wetland component gives a prediction that is not significantly different from a prediction made with the site-specific classes. If the forested wetland is not included, the total water flux is under-predicted by more than half when there is high evaporative demand.

Conclusions

Our results show that leaf area, while a necessary input for regional to global scale models, is insufficient for characterizing ecosystem processes even within broad biome classifications. An accurate determination of species contribution to water fluxes is important. For northern Wisconsin, a distinction is needed between aspen and hardwoods, which is attainable from high resolution remote sensing using conventional classification techniques. These differences are expected to significantly alter the results of models of gas exchange, including carbon uptake by the forests. This result is supportive of the use of distribution functions to account for species mixtures within coarse resolution remote sensing pixels or grids used in mesoscale and atmospheric GCM models. However, a second important conclusion is that the presence of significant wetland can offset the lack of data on variable stomatal physiologies when trying to predict total daily water fluxes from the landscape during wet periods. This may allow large-scale models to accurately predict water and energy fluxes at daily or longer timescales in northern Wisconsin with only rudimentary forest physiological detail. However, the proportion of forested wetland vs. upland forest must be known, and this is currently not obtainable from coarse resolution satellite data. Future regional to global scale studies should consider ways of incorporating these hydrologically significant land surface properties into models, by integrating high-resolution satellite imagery, soils, and topography into land surface parameterizations.

Acknowledgements

This research was supported primarily by the Land Surface Hydrology Program of the National Aeronautics and Space Administration, through grant #NAG5-8554. We are indebted to Eric Wood and Dennis Lettenmaier for establishing this program. Additional support of this research was provided through McIntire-Stennis funding. Numerous undergraduate students are thanked for assisting with data collection and processing. Funding for WLEF flux measurements were provided by the National Institute for Global Environmental Change through the U.S. Department of Energy. The Atmospheric Chemistry Project of the Climate and Global Change Program of the National Oceanic and Atmospheric Administration supported site infrastructure and maintenance. The WLEF work would not be possible without the cooperation of the Wisconsin Educational Communications Board and Roger Strand (chief engineer for WLEF-TV). We are grateful to Mark Friedl, an anonymous reviewer, and the Subject Editor, whose comments and suggestions improved the manuscript.

References

Ahl DE (2002) A Measurement and Modeling Perspective on Requirements for Future Remote Sensing Vegetation Indices and Classifications, Unpublished PhD Dissertation, Environmental Monitoring, Institute for Environmental Studies, University of Wisconsin, Madison, 181pp.

Avissar R, Pielke RA (1991) The impact of plant stomatal control on mesoscale atmospheric circulations. *Agricultural and Forest Meteorology*, **54**, 353–372.

Bakwin PS, Tans PP, Hurst DF *et al.* (1998) Measurements of carbon dioxide on very tall towers: Results of the NOAA/CMDL program. *Tellus Series B-Chemical and Physical Meteorology*, **50**, 401–415.

Baldocchi DD, Law BE, Antoni PM (2000) On measuring and modeling energy fluxes above the floor of a homogeneous and heterogeneous conifer forest. *Agricultural and Forest Meteorology*, **102**, 187–206.

Bauer ME, Burk TE, Ek AR *et al.* (1994) Satellite inventory of Minnesota forest resources. *Photogrammetric Engineering and Remote Sensing*, **60**, 287–298.

Berger BW, Davis KJ, Yi C *et al.* (2001) Long-term carbon dioxide fluxes from a very tall tower in a northern forest: Flux measurement methodology. *Journal of Atmospheric and Oceanic Technology*, **18**(4), 529–542.

Brannon DP, Hill CL, Davis BA *et al.* (1994) Commercial remote sensing program. *Photogrammetric Engineering and Remote Sensing*, **60**, 317–330.

Burrows SN, Gower ST, Clayton MK *et al.* (2002) Application of geostatistics to characterize LAI from flux towers to landscape scales using a cyclic sampling design. *Ecosystems*, in press.

Camillo PJ, Gurney RJ (1986) A resistance parameter for bare-soil evaporation models. *Soil Science*, **141**, 95–105.

Campbell JL, Burrows S, Gower ST *et al.* (1999) *Bigfoot: Characterizing Land Cover, LAI, and NPP at the Landscape Scale for EOS/MODIS Validation*. Field Manual, Version 2.1, Environmental Sciences Division, Oak Ridge National Laboratory, Oak Ridge, TN, 104pp.

Campbell GS, Norman JM (1998) *An Introduction to Environmental Biophysics*, 2nd edn. Springer, New York.

Chen J, Rich PW, Gower ST *et al.* (1997) Leaf area index of boreal forests: Theory, techniques and measurements. *Journal of Geophysical Research*, **102**(D24), 29 429–29 433.

Clapp R, Hornberger G (1978) Empirical equations for some soil hydraulic properties. *Water Resources Research*, **14**, 601–604.

Daamen CC, Simmonds LP (1996) Measurement of evaporation from bare soil and its estimation using surface resistance. *Water Resources Research*, **32**, 1393–1402.

Davis KJ, Bakwin PS, Yi C *et al.* (2002) The annual cycles of CO_2 and H_2O exchange over a northern mixed forest as observed from a very tall tower. *Global Change Biology* (in press).

Deardorff JW (1978) Efficient prediction of ground temperature and moisture with inclusion of a layer of vegetation. *Journal of Geophysical Research*, **83**, 1889–1903.

DeFries RS, Hansen MC, Townshend JRG (2000) Global continuous fields of vegetation characteristics: a linear mixture model applied to multi-year 8 km AVHRR data. *International Journal of Remote Sensing*, **21**, 1389–1414.

Dickinson RE (1984) *Modeling Evapotranspiration for Three-Dimensional Climate Models*. In: (eds Hansen JE, Takahashi T), eds. Climate Processes and Climate Sensitivity. Geophysical Monographs Series, 29, American Geophysical Union, Washington, D.C., 58–72.

Dickinson RE, Shaikh M, Bryant R *et al.* (1998) Interactive canopies in a climate model. *Journal of Climate*, **11**, 2823–2836.

Entekhabi D, Eagleson P (1989) Land surface hydrology parameterization for atmospheric general circulation models including subgrid variability. *Journal of Climate*, **2**, 816–831.

Ewers BE, Mackay DS, Gower ST *et al.* (2002) Tree species effects on stand transpiration in northern Wisconsin. *Water Resources Research*, in press.

Ewers BE, Oren R (2000) Analysis of assumptions and errors in the calculation of stomatal conductance from sap flux measurements. *Tree Physiology*, **20**, 579–589.

Ewers BE, Oren R, Albaugh TJ *et al.* (1999) Carry-over effects of water and nutrient supply on water use of Pinus taeda. *Ecological Applications*, **9**(2), 513–525.

Ewers BE, Oren R, Sperry JS (2000) Influence of nutrient versus water supply on hydraulic architecture and water balance in Pinus taeda. *Plant, Cell, and Environment*, **23**, 1055–1066.

Falge E, Baldocchi D, Olson R *et al.* (2001) Gap filling strategies for long term energy flux data sets. *Agricultural and Forest Meteorology*, **107**, 71–77.

Fassnacht KS, Gower ST (1997) Interrelationships among edaphic and stand characteristics, leaf area index, and aboveground net primary productivity for upland forest ecosystems in north central Wisconsin. *Canadian Journal of Forest Research*, **27**, 1058–1067.

Fassnacht KS, Gower ST (1999) Comparison of the litterfall and forest floor organic matter and nitrogen dynamics of upland forest ecosystems in north central Wisconsin. *Biogeochemistry*, **43**, 265–284.

Foley JA, Levis S, Costa MH *et al.* (2000) Incorporating dynamic vegetation cover within global climate models. *Ecological Applications*, **10**(6), 1620–1632.

Foley JA, Prentice IC, Ramankutty N *et al.* (1996) An integrated biosphere model of land surface processes, terrestrial carbon balance, and vegetation dynamics. *Global Biogeochemical Cycles*, **10**(4), 603–628.

Franklin J, Woodcock CE (1997) Multiscale vegetation data for the mountains of Southern California: Spatial and categorical resolution. In: *Scaling in Remote Sensing and GIS* (eds Quattrochi, DA, Goodchild, MF), pp. 141–168. Lewis Publishers, Boca Raton, FL.

Gower ST, Kucharik CJ, Norman JM (1999) Direct and indirect estimation of leaf area index, f_{APAR}, and net primary productivity of terrestrial ecosystems. *Remote Sensing of Environment*, **70**, 29–51.

Gower ST, Norman JM (1991) Rapid estimation of leaf area index in conifer and broad-leaf plantations. *Ecology*, **72**, 1896–1900.

Granier A (1987) Evaluation of transpiration in a Douglas fir stand by means of sap flow measurements. *Tree Physiology*, **3**, 309–320.

Jarvis PG (1976) The interpretation of the variations in leaf water potential and stomatal conductance found in canopies in the field. *Philosophical Transactions of the Royal Society of London B*, **273**, 593–610.

Lillesand TM, Keifer RW (2000) *Remote Sensing and Image Interpretation*. John Wiley & Sons, Inc., New York.

Loveland TR, Belward AS (1997) The IGBP-DIS global 1-km land cover data set, DISCover: First Results. *International Journal of Remote Sensing*, **18**, 3289–3295.

Mackay DS (2001) Evaluation of hydrologic equilibrium in a mountainous watershed: Incorporating forest canopy spatial adjustment to soil biogeochemical processes. *Advances in Water Resources*, **24**, 1211–1227.

Mackay DS, Band LE (1997) Forest ecosystem processes at the watershed scale: dynamic coupling of distributed hydrology and canopy growth. *Hydrological Processes*, **11**, 1197–1217.

Mahfouf JF, Noilhan J (1991) Comparative study of various formulations of evaporation from bare soil using *in situ* data. *Journal of Applied Meteorology*, **30**, 1354–1365.

McNaughton KG, Jarvis PG (1991) Effects of spatial scale on stomatal control of transpiration. *Agricultural and Forest Meteorology*, **54**, 279–301.

Meinzer FC, Goldstein G, Andrade JL (2001) Regulation of water flux through tropical canopy trees: Do universal rules apply? *Tree Physiology*, **21**, 19–26.

Moncrieff JB, Malhi Y, Leuning R (1996) The propagation of errors in long-term measurements of land–atmosphere fluxes of carbon and water. *Global Change Biology*, **2**, 231–240.

Monteith JL (1995) A reinterpretation of stomatal response to humidity. *Plant, Cell and Environment*, **18**, 357–364.

Moody A (1998) Using landscape spatial relationships to improve estimates of land-cover area from coarse resolution remote sensing. *Remote Sensing of Environment*, **64**, 202–220.

Oren R, Phillips N, Katul G *et al.* (1998) Scaling xylem sap flux and soil water balance, and calculating variance: a method for partitioning water flux in forests. *Annales des Sciences, Forestieres*, **55**, 191–216.

Oren R, Sperry JR, Katul GG *et al.* (1999) Survey and synthesis of intra- and interspecific variation in stomatal sensitivity to vapour pressure deficit. *Plant, Cell and Environment*, **22**, 1515–1526.

Pan HL, Mahrt L (1987) Interaction between soil hydrology and boundary layer development. *Boundary Layer Meteorology*, **38**, 185–202.

Pauwels VRN, Wood EF (2000) The importance of classification differences and spatial resolution of land cover data in the uncertainty in model results over Boreal ecosystems. *Journal of Hydrometeorology*, **1**, 255–266.

Phillips N, Oren R (1998) A comparison of daily representations of canopy conductance based on two conditional time-averaging methods. *Annales des Sciences Forestiers*, **55**, 191–216.

Pielke RA, Avissar R (1990) Influence of landscape structure on local and regional climate. *Landscape Ecology*, **4**(2/3), 133–155.

Running SW, Hunt ER Jr. (1993) Generalization of a forest ecosystem process model for other biomes, BIOME-BGC, and application for global scale models. In: *Scaling Physiological Processes: Leaf to Globe* (eds Ehleringer JR, Field CB), pp. 141–158. Academic Press, San Diego, CA.

Running SW, Loveland TR, Pierce LL *et al.* (1995) A remote sensing based vegetation classification logic for global land cover analysis. *Remote Sensing of Environment*, **51**, 39–48.

Sauer TJ, Hatfield JL, Prueger JH (1996) Aerodynamic characteristics of standing corn stubble. *Agronomy Journal*, **88**(5), 733–739.

Sellers PJ, Los SO, Tucker CJ *et al.* (1996) A revised land surface parameterization (SiB2) for atmospheric GCMs. Part II: The generation of global fields of terrestrial biophysical parameters from satellite data. *Journal of Climate*, **9**, 676–705.

Sellers P, Mintz Y, Sud Y *et al.* (1986) A simple biosphere model (SiB) for use within general circulation models. *Journal of Atmospheric Science*, **43**, 505–531.

Sperry JS, Adler FR, Campbell GS *et al.* (1998) Limitation of plant water use by rhizosphere and xylem conductance: Results from model. *Plant, Cell and Environment*, **21**, 347–359.

Stuckens J, Coppin PR, Bauer ME (2000) Integrating contextual information with per-pixel classification for improved land cover classification. *Remote Sensing of Environment*, **71**, 282–296.

Thomlinson JR, Bolstad PV, Cohen WB (1999) Coordinating methodologies for scaling landcover classifications from site-specific to global: Steps toward validating global map products. *Remote Sensing of Environment*, **70**, 16–28.

Waddington JM, Roulet NT (2000) Carbon balance of a boreal patterned peatland. *Global Change Biology*, **6**, 87–97.

WiDNR (1998) *GEODISC 3.0*. Wisconsin Department of Natural Resources, Geographic Services Section, October, 1998.

Wolter PT, Mladenoff DJ, Host GE *et al.* (1995) Improved forest classification in the northern lake states using multi-temporal Landsat imagery. *Photogrammetric Engineering and Remote Sensing*, **61**(9), 1129–1143.

Wood EF, Lettenmaier DP, Zartarian V (1992) A land surface hydrology parameterization with sub-grid variability for general circulation models. *Journal of Geophysical Research*, **97**(D3), 2717–2728.

Xue Y, Fennessey M, Sellers P (1996) Impact of vegetative properties on U.S. summer weather prediction. *Journal of Geophysical Research*, **101**, 7419–7430.

Zeng X, Dickinson RE, Walker A *et al.* (2000) Derivation and evaluation of global 1-km fractional vegetation cover data for land modeling. *Journal of Applied Meteorology*, **39**, 826–839.